

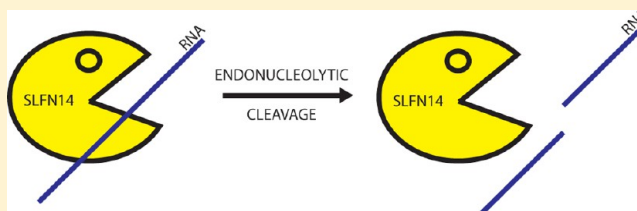
## Characterization of Novel Ribosome-Associated Endoribonuclease SLFN14 from Rabbit Reticulocytes

Vera P. Pisareva,<sup>\*,†</sup> Ilham A. Muslimov,<sup>‡</sup> Andrew Tcherepanov,<sup>‡</sup> and Andrey V. Pisarev<sup>\*,†</sup>

<sup>†</sup>Department of Cell Biology and <sup>‡</sup>Department of Physiology and Pharmacology, SUNY Downstate Medical Center, 450 Clarkson Avenue, Brooklyn, New York 11203, United States

### Supporting Information

**ABSTRACT:** Turnover of mRNA is a critical step that allows cells to control gene expression. Endoribonucleases, enzymes cleaving RNA molecules internally, are some of the key components of the degradation process. Here we provide a detailed characterization of novel endoribonuclease SLFN14 purified from rabbit reticulocyte lysate. Schlafen genes encode a family of proteins limited to mammals. Their cellular function is unknown or incompletely understood. In reticulocytes, SLFN14 is strongly overexpressed, represented exclusively by the short form, all tethered to ribosomes, and appears to be one of the major ribosome-associated proteins. SLFN14 binds to ribosomes and ribosomal subunits in the low part of the body and cleaves RNA but preferentially rRNA and ribosome-associated mRNA. This results in the degradation of ribosomal subunits. This process is strictly  $Mg^{2+}$ - and  $Mn^{2+}$ -dependent, NTP-independent, and sequence nonspecific. However, in other cell types, SLFN14 is a full-length solely nuclear protein, which lacks ribosomal binding and nuclease activities. Mutational analysis revealed the ribosomal binding site and the aspartate essential for the endonucleolytic activity of protein. Only few endoribonucleases participating in ribosome-mediated processes have been characterized to date. Moreover, none of them are shown to be directly associated with the ribosome. Therefore, our findings expand the general knowledge of endoribonucleases involved in mammalian translation control.



Eukaryotic cells have created multiple highly regulated and complex mechanisms to control the level of particular cytoplasmic messenger RNA (mRNA) molecules, ensuring their functionality and providing their degradation in the case of incorrect transcript maturation, some stress stimuli, or the accomplishment of cellular function. mRNA degradation is mediated through several pathways. RNA quality control starts in the nucleus and covers the transcription and processing stages. Aberrant mRNAs, which escaped into the cytoplasm, are identified on the basis of the translation process and destroyed by different surveillance machineries depending on the type of abnormality. The concentration of fully matured mRNAs is, in turn, regulated by the RNA interference mechanism in addition to the general mRNA turnover process. Although mRNA degradation in prokaryotes is initiated by endoribonucleases, it was widely accepted that eukaryotes employ for the decay mostly exoribonucleases, enzymes hydrolyzing the RNA molecule from 5'- and 3'-ends. Currently, the growing number of reports of identified and suggested endoribonucleases assigns a key role in various degradation pathways to these enzymes. According to current opinion, the mRNA molecule after the initial internal cleavage is subsequently degraded by exoribonucleases.<sup>1,2</sup>

Endoribonucleases reveal a great variety in the organization of the active center and, therefore, are structurally diverse. Only some of them (for example, RNase L and IRE1) share the similar nuclease domain composition and catalytic mechanisms.<sup>3</sup> Moreover, the nuclease domains of many known

endoribonucleases (for example, PMR1, APE1, and adolase C) have yet to be identified.<sup>1</sup> As a result, it is very difficult to predict novel endoribonucleases based on the primary sequence comparative analysis. Thus, the enzymes responsible for many processes relying on the internal cleavage of RNA (for example, no-go decay and 18S nonfunctional rRNA decay) are still unknown.

The intracellular distribution of endoribonucleases is one of the options for controlling RNA target specificity. Endoplasmic reticulum (ER)-anchored IRE1 is a good example for providing such localized degradation activity. After the response of the unfolded protein, which is a cellular response associated with the accumulation of unfolded or misfolded proteins in the lumen of the ER, IRE1 initiates the cleavage of ER-localized mRNAs to cease the translation and, therefore, mediates the recovery from stress.<sup>4</sup> Interestingly, the vast majority of endoribonucleases seems to act in the cytoplasm, because they are found to be enriched in such cytoplasmic components as stress granules (sites for mRNA storage and degradation), exosomes (RNA degradation protein machineries), RNA-induced silencing complex (RISC, part of the RNA interference pathway), and polysomes.<sup>1,2</sup> Importantly, some of them become redistributed in the cytoplasm to mediate the response

Received: March 19, 2015

Revised: May 5, 2015

Published: May 21, 2015

of the cell to different stimuli. For example, PMR1 endoribonuclease is found to be associated with polysomes, but it is transferred to stress granules upon arsenite treatment.<sup>5,6</sup>

Another significant characteristic of endoribonucleases is their specificity for mRNA targets. Some enzymes are involved in the general degradation mechanism such as RNA interference (Dicer and AGO2) and mRNA surveillance (SMG6) pathways, where they cut mRNAs in a nonspecific manner. Others cleave particular mRNAs and, therefore, play an essential role in their metabolism. For instance, Ard-1, G3BP, and APE1 endoribonucleases have been shown to regulate c-myc mRNA, which encodes the transcription factor and whose turnover should be tightly controlled.<sup>7-9</sup>

In our laboratory, we investigate the mammalian translation process by reconstituting it *in vitro* from purified components. Although the mechanism of canonical stages (initiation, elongation, termination, and ribosomal recycling) has been well-studied, the details of numerous regulation steps remain unknown. Recently, we became interested in mRNA surveillance pathways, which take place in the cytoplasm and absolutely depend on the translation cycle. These pathways aim to destroy mRNAs, which cannot be correctly translated: nonsense-mediated decay (NMD) targets mRNAs with a premature termination codon, no-go decay (NGD) eliminates transcripts containing the elements in the open reading frame arresting the ribosome during the elongation step, and nonstop decay (NSD) degrades mRNAs without a termination codon.<sup>10-12</sup> Genetic experiments in yeast revealed the endonucleolytic cleavage of mRNA in the proximity of a structured barrier during NGD.<sup>13</sup> To determine the unknown endoribonuclease involved in NGD, we employed an *in vitro* reconstitution approach for assembling the stalled ribosomal elongation complex on a model mRNA coupled with the rabbit reticulocyte lysate (RRL) fractionation. The purified enzyme was identified as SLFN14, a member of the Schlafen protein family that is limited to mammals. Although SLFN14 introduced the endonucleolytic cleavage to mRNA downstream of the P site of the ribosome, its abundance in RRL resulting in the complete rRNA degradation and independence of catalytic activity from translation machinery raise the question of the authentic role of SLFN14 in the cell. It was found that the expression level of *Slfn1*, which was the first member of the Schlafen family discovered, has a profound effect on cell growth and progression through the cell cycle. In particular, overexpression of *Slfn1* resulted in a cell cycle arrest at the G<sub>0</sub>/G<sub>1</sub> stage. Therefore, the family had been named *Schlafen*, which is translated from German as “to sleep”.<sup>14</sup> Consistently, with the aforementioned diversity among members of this class of enzymes, it is not surprising that SLFN14 does not share sequence and structural homology with any described eukaryotic endoribonucleases. However, the detailed biochemical characterization of protein and mutational analysis unambiguously confirmed that SLFN14 is a bona fide endoribonuclease with yet-to-be-identified cellular function.

## MATERIALS AND METHODS

**Antibodies.** SLFN14, GAPDH, HDAC2, and eIF2 $\alpha$  antibodies were from Abcam.

**Purification of Translation Factors, Ribosomal Subunits, and Aminoacylation of tRNA.** Native 40S and 60S subunits, DHX29, ABCE1, eIF 2, 3, 4F, and 5B, eEF 1H and 2, recombinant eIF 1, 1A, 3j, 4A, 4B, and 5, and eRF 1 and 3 were

purified as described previously.<sup>15,16</sup> Rabbit aminoacyl-tRNA synthetases were purified, and *in vitro* transcribed tRNA<sub>i</sub><sup>Met</sup>, tRNA<sup>Val</sup>, and rabbit native total tRNAs (Promega) were aminoacylated as appropriate, as described previously.<sup>16</sup>

**SLFN14 Purification.** Native rabbit SLFN14 was purified from RRL on the basis of endonucleolytic cleavage of HBBmod mRNA in assembled *in vitro* stalled EC. Native murine SLFN14 was purified from Krebs ascites cell lysate on the basis of chasing the protein by immunoblotting. Purification of both forms involved preparation of ribosomal salt wash, fractionation by ammonium sulfate precipitation, chromatography on DEAE cellulose and phosphocellulose, and FPLC on MonoS/MiniS, MonoQ, and hydroxyapatite columns, as appropriate. Recombinant rabbit and murine forms of SLFN14–65kDa were expressed in *Escherichia coli* and isolated by affinity chromatography on Ni-NTA agarose followed by affinity purification on 80S ribosomes via SDG centrifugation. Recombinant rabbit SLFN14–45kDa and its mutants were expressed in *E. coli* and isolated by affinity chromatography on Ni-NTA agarose followed by FPLC on a MonoS column.

**ATPase Assay.** SLFN14 was incubated with [ $\gamma$ -<sup>32</sup>P]ATP in the presence or absence of (CU)<sub>17</sub> RNA, 40S ribosomal subunits, and 80S ribosomes. Reaction mixtures were analyzed by chromatography on PEI cellulose.

**Analysis of SLFN14's Association with Ribosome and Ribosomal Subunits.** Different forms of SLFN14 were incubated with 40S subunits, 60S subunits, or 80S ribosomes in the presence or absence of AMPPNP or ADP and subjected to centrifugation through 10–30% SDG. Fractions that corresponded to ribosomal complexes were resolved via NuPAGE 4–12% Bis-Tris SDS–PAGE (Invitrogen) and stained with SimplyBlue SafeStain (Invitrogen) or tested with anti-SLFN14 antibodies, as indicated.

**rRNA Degradation.** To study rRNA degradation in lysates, RRL or HEK293T cell extract was incubated in the presence of ATP and GTP for different periods of time. To compare rRNA degradation in RRL and 80S/SLFN14 binary system, 80S ribosomes were incubated with SLFN14 in the presence of ATP and GTP. To investigate rRNA degradation of purified ribosomal subunits, 40S or 60S subunits were incubated with SLFN14 in the presence of ATP and GTP. To test the endonucleolytic activity of SLFN14 in the ribosome-bound state, aforementioned SDG-purified 80S/SLFN14 complexes or 80S ribosomes were incubated at 37 °C and assayed. To compare the endonucleolytic activity of rabbit and murine native forms of SLFN14 in the degradation of 18S rRNA, proteins were incubated with 40S subunits. After incubation, RNA was isolated and analyzed by DAFGE or denaturing PAGE, as appropriate.

**mRNA and tRNA Degradation.** The 5'-end <sup>32</sup>P-labeled HBBmod mRNA, GUSmod mRNA, tRNA<sup>His</sup>, or tRNA<sup>Val</sup> was incubated with SLFN14 in the presence of ATP for different periods of time. To study the dependence of SLFN14 on metal ions with respect to cleavage activity, SLFN14 was incubated with 5'-end <sup>32</sup>P-labeled GUSmod mRNA in the presence of ATP and 1 mM metal ion, as appropriate. After incubation, RNA was isolated and resolved via 6% denaturing PAGE. Gels were dried and autoradiographed.

**Analysis of Ribosome and Ribosomal Subunit Integrity after rRNA Degradation.** To test the integrity of the ribosome and ribosomal subunits after rRNA cleavage in the binary system, 80S ribosomes or 40S or 60S subunits were incubated in the presence or absence of SLFN14 and subjected



to centrifugation via 10–30% SDG. To study the integrity of 80S monosomes and polysomes after RNA cleavage in lysate, RRL after incubation in the presence of ATP, GTP, and CHX or without incubation was subjected to centrifugation via 10–50% SDG. After centrifugation, the rRNA appearance and protein content of 80S complex fractions were assayed by DAFGE and SDS–PAGE, respectively.

**Functional Activity of rRNA-Cleaved Ribosomes in the Translation Cycle.** To compare the activity of cleaved and intact ribosomes in the formation of 80S initiation complexes, the Met-Puro assay was employed essentially as described previously.<sup>17</sup> MVHL-STOP mRNA, eIFs 1, 1A, 2, 3, 4A, 4B, 4F, 35S-labeled Met-tRNA<sup>Met</sup>, and intact or cleaved 40S subunits were incubated in the presence of ATP and GTP, supplemented with eIF5, eIF5B, and intact or cleaved 60S subunits, as appropriate, and additionally incubated. After assembly, ribosomal complexes were treated with puromycin and extracted with ethyl acetate. <sup>35</sup>S-labeled methionyl-puromycin formation was measured by scintillation counting of the ethyl acetate extract. To compare the activity of cleaved and intact ribosomes in the entire translation cycle, different stages of translation, initiation, elongation, termination, and ribosomal recycling, were reconstituted *in vitro* from individual purified components and assayed by toeprint essentially as described previously.<sup>16</sup>

**RRL Ribosomal Profile Preparation.** Flexi RRL supplemented with 70 mM KCl and 1 mM GMPPNP was incubated and subjected to centrifugation via 10–30% SDG. Fractions (200  $\mu$ L) were collected. Ribosomes and ribosomal subunit-containing fractions were determined by the analysis of their rRNA content via DAFGE.

**SLFN14 Protein Level and Localization in Cells.** To test the distribution of SLFN14 in the RRL ribosomal profile, SDG fractions were subjected to SDS–PAGE and assayed by immunoblotting. To calculate the SLFN14:80S ribosome ratio, the 80S complex and different amounts of purified SLFN14 were subjected to SDS–PAGE and assayed by immunoblotting. To estimate the prevalence of SLFN14 among 80S ribosome-associated proteins in RRL, the 80S complex fraction after RRL ribosomal profiling was subjected to SDS–PAGE and stained with SimplyBlue SafeStain. To compare the SLFN14 protein level in RRL and different rabbit tissue lysates, 40  $\mu$ g of total protein of RRL from two different sources (Promega and Green Hectares) and brain, lung, and liver rabbit tissue lysates were subjected to SDS–PAGE and assayed by immunoblotting with anti-SLFN14 and anti-eIF2 $\alpha$  (loading control) antibodies. To determine the distribution of SLFN14 between the nucleus and cytoplasm in cells, 40  $\mu$ g of total protein of nuclear or cytoplasmic extracts of HEK293T or MCF7 cells was subjected to SDS–PAGE and assayed by immunoblotting with anti-SLFN14, anti-HDAC2 (nuclear marker), and anti-GAPDH (cytoplasmic marker) antibodies.

**Endonucleolytic Activity of Different Recombinant Forms of SLFN14.** After affinity purification of SLFN14–65kDa on 80S ribosomes by centrifugation through SDG, the 80S/SLFN14–65kDa complex, 80S/empty vector expression complex, and empty 80S ribosome were incubated, and rRNA degradation was assayed by DAFGE. To test the endonucleolytic activity of SLFN14–45kDa and its mutants, proteins were incubated with 5'-end <sup>32</sup>P-labeled HBBmod mRNA in the presence or absence of 1 mM Mg<sup>2+</sup> ions, as indicated. After incubation, RNA was isolated and resolved via 6% denaturing PAGE. Gels were dried and autoradiographed.

### Sequence and Structure Specificity of SLFN14 in Cleavage of Free and Ribosome-Associated mRNA.

To test the sequence and structure specificity of SLFN14 in the cleavage of free mRNA, SLFN14 was incubated with GUSmod mRNA or HBBmod mRNA, mRNA was isolated, and cleavage sites were determined by AMV reverse transcriptase-mediated extension of <sup>32</sup>P-labeled primer complementary to mRNA. cDNA products were resolved via 6% denaturing PAGE. To compare the site specificity of SLFN14 in the cleavage of free and ribosome-associated mRNA, 80S initiation and elongation complexes were assembled on HBBmod mRNA *in vitro* from individual purified components, purified by SDG centrifugation, and analyzed by toeprint as described previously.<sup>16</sup> SDG-purified complexes were incubated with SLFN14, and mRNA was isolated and assayed by primer extension.

**Ribosomal Position of SLFN14.** 40S subunits were incubated with SLFN14. Cleavage sites in 18S rRNA were identified by the extension of corresponding primers complementary to rabbit 18S rRNA.

## RESULTS

### SLFN14 Protein Is Responsible for the Endonucleolytic Cleavage of RNA in RRL.

Before starting the RRL fractionation search of the unknown endoribonuclease involved in NGD, we assembled the stalled ribosomal elongation complex (stalled EC) in an *in vitro* reconstituted system on a model mRNA and purified it by centrifugation through the sucrose density gradient (SDG). Model “HBBmod” mRNA comprises the  $\beta$ -globin 5'-untranslated region (5'-UTR) and nonapeptide-encoding open reading frame (ORF) followed by a stem structure of 27 nucleotide base pairs (Figure 1A). This stem was successfully employed for the assembly of stalled EC and the detection of NGD-associated endonucleolytic cleavage of mRNA in yeast.<sup>13</sup> The efficient formation of purified stalled EC was confirmed by a toeprint assay. According to this technique, the ribosomal complex on mRNA yields a toeprint signal at its leading edge. Our reconstituted complexes revealed toeprint signals located at the beginning of a stem, indicating that they are true stalled ECs (in Figure 1B, compare lanes 1 and 2). To detect endonucleolytic cleavage, stalled EC was incubated with RRL or its ribosomal salt wash (RSW) and mRNA was isolated and assayed by primer extension. Although we did not observe any changes after incubation with RRL (Figure 1B, lane 4), strong cleavage was found after incubation with RSW within the stem, a few nucleotides downstream of the stalled EC toeprint signal (Figure 1B, lane 3), suggesting the enrichment of the responsible endoribonuclease in the ribosome-associated fraction of proteins. We could not identify the precise position of cleavage because of the nucleotide sequence compression in this area of the stem. To isolate the endoribonuclease activity, we undertook protein purification from RSW of RRL employing the combination of different fractionation techniques coupled with testing of intermediate fractions for mRNA cleavage of stalled EC. Mass spectrometry of the final protein at 99% purity in the fraction identified it as a C-terminally truncated form (approximately 95kDa) of SLFN14 (the full-length rabbit form is 114kDa) (Figure 1C). The short form of the protein may result from alternative mRNA splicing or proteolytic cleavage of full-length SLFN14 specifically in reticulocytes. SLFN14 belongs to the Schlafen protein family found in mammals and encoded by six *Slfn* genes in humans. All SLFN proteins share a highly conserved N-terminus containing a putative AAA domain involved in ATP

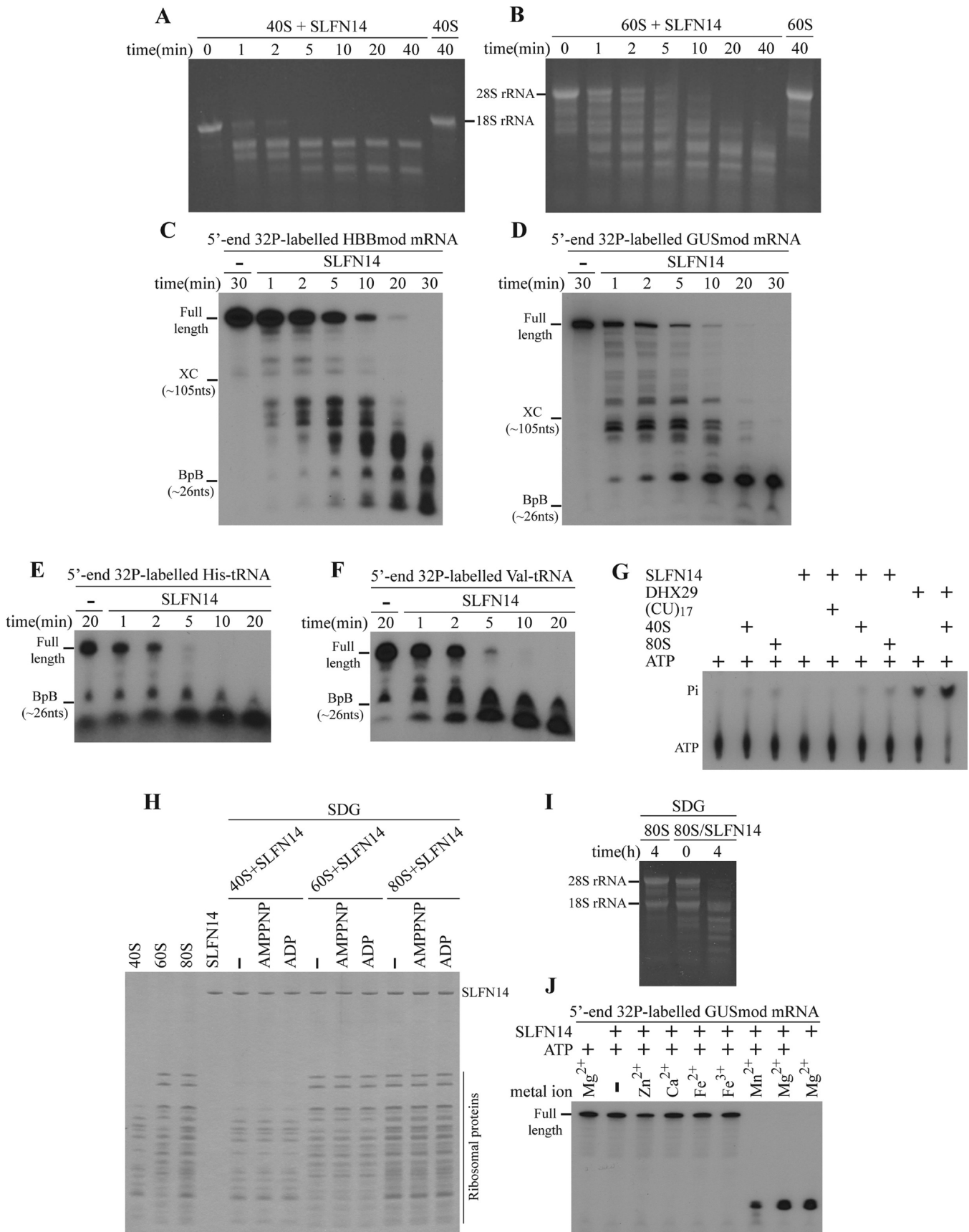


**Figure 2.** SLFN14 binds the ribosome and ribosomal subunits and cleaves different types of RNA in a Mg<sup>2+</sup>- and Mn<sup>2+</sup>-dependent and ATP-independent manner. (A and B) Kinetics of degradation of rRNA by SLFN14 in purified 40S subunits and 60S subunits, respectively, assayed by DAFGE. (C–F) Kinetics of degradation of 5'-end <sup>32</sup>P-labelled HBBmod mRNA, GUSmod mRNA, His-tRNA, and Val-tRNA, respectively, by SLFN14 analyzed by denaturing PAGE. (G) Thin layer chromatography analysis of SLFN14's ATPase activity in the presence or absence of (CU)<sub>17</sub>

Figure 2. continued

RNA, 40S subunits, or 80S ribosomes. DHX29 helicase (positive control) is ATPase; its hydrolyzing activity is stimulated by 40S subunits. Positions of [ $\gamma$ - $^{32}$ P]ATP and [ $^{32}$ P]P<sub>i</sub> are indicated. (H) Association of SLFN14 with 80S ribosomes or 40S and 60S subunits in the presence or absence of nucleotides, as indicated, assayed by SDG centrifugation and SDS-PAGE of peak ribosomal fractions. (I) rRNA degradation in the SDG-purified 80S/SLFN14 complex before or after incubation tested by DAFGE. (J) Dependence of SLFN14 endonucleolytic activity on metal ions and ATP analyzed by denaturing PAGE.

binding,<sup>18,19</sup> whereas only long *Sfn* genes (including *Sfn14*) possess a C-terminal extension with motives found in superfamily I DNA/RNA helicases.<sup>18</sup> Members of this family are involved in an antiviral immune response,<sup>20</sup> differentiation,<sup>21</sup> and T-cell development.<sup>14,18,22</sup>

To confirm our finding, stalled EC was incubated with native SLFN14. We observed a similar cleavage of mRNA as in the presence of RSW (Figure 1D, lanes 1 and 2, empty triangle). Surprisingly, the incubation of HBBmod mRNA alone, not in the stalled EC, with SLFN14 resulted in multiple additional endonucleolytic cleavages distributed along mRNA (Figure 1D, lanes 3 and 4, filled triangles), suggesting that the activity of SLFN14 is independent of the ribosome. Because SLFN14 alone manifests the activity and, at the same time, is enriched with RSW, we tested the potential effect of SLFN14 on the degradation of rRNA in RRL. In contrast to HEK293T (human embryonic kidney) cell extract, RRL incubation at 37 °C within 12 h resulted in a complete endonucleolytic cleavage of 28S rRNA as revealed via denaturing agarose/formaldehyde gel electrophoresis (DAFGE), whereas 18S rRNA degraded much slower (Figure 1E). To confirm the role of SLFN14 in the degradation of rRNA, we assayed the protein with purified rabbit 80S ribosomes. Incubation of SLFN14 with 80S ribosomes in an equimolar ratio demonstrated a final rRNA degradation pattern identical to that of RRL (Figure 1F). The slightly different initial pattern could be explained by the protection of the ribosome with ribosome-associated proteins in RRL. Thus, although SLFN14 causes the endonucleolytic cleavage of mRNA in stalled EC, a role more general than the initially suggested role in the NGD process cannot be ruled out.

**SLFN14 Specifically Binds the Ribosome and Ribosomal Subunits and Cleaves Different Types of RNA in a Mg<sup>2+</sup>- and Mn<sup>2+</sup>-Dependent and ATP-Independent Manner.** To test whether SLFN14 cleaves rRNA in individual ribosomal subunits, we incubated purified 40S or 60S subunits with the excess of isolated SLFN14 to accelerate degradation kinetics and analyzed RNA via DAFGE. Again, we observed a characteristic endonucleolytic cleavage pattern (Figure 2A,B). To examine the universality of the process, we used 5'-end <sup>32</sup>P-labeled mRNA and tRNA transcripts. Randomly chosen modified  $\beta$ -glucuronidase (GUSmod) and already described HBBmod mRNAs as well as His-tRNA and Val-tRNA after incubation with SLFN14 revealed endonucleolytic cleavage patterns in denaturing polyacrylamide gel electrophoresis (PAGE) (Figure 2C–F). Therefore, SLFN14 degrades different types of cellular RNA in a binary system.

Because SLFN14 harbors the AAA domain, we studied its ATPase activity by thin layer chromatography. Interestingly, SLFN14 contains the truncated 129-amino acid AAA domain, compared to the 200–250-amino acid regular one. Importantly, some AAA proteins are inactive as ATPases, and some do not even bind ATP. Therefore, it is not surprising that SLFN14 did not hydrolyze [ $\gamma$ - $^{32}$ P]ATP and hydrolysis was not stimulated by (CU)<sub>17</sub> RNA, 40S ribosomal subunits, or 80S ribosomes (Figure 2G). To investigate the interaction of SLFN14 with the

ribosome, we mixed SLFN14 with 40S or 60S subunits or 80S ribosomes in the presence of AMPPNP or ADP and in the absence of a nucleotide without incubation to prevent degradation and purified complexes by SDG centrifugation. SLFN14 efficiently bound to the ribosome and ribosomal subunits in a nucleotide-independent manner (Figure 2H). Following incubation of such SDG-purified 80S/SLFN14 complexes caused rRNA degradation (Figure 2I). The activity of several characterized endoribonucleases (for example, RNase L, Dicer, Ago2, and SMG6) depends on Mg<sup>2+</sup> and Mn<sup>2+</sup> ions.<sup>1</sup> Consistently, SLFN14 cleaved GUSmod mRNA in the binary system in the presence of Mg<sup>2+</sup> or Mn<sup>2+</sup>, but not Zn<sup>2+</sup>, Ca<sup>2+</sup>, Fe<sup>2+</sup>, or Fe<sup>3+</sup> ions, and the activity was ATP-independent (Figure 2J).

To confirm the accuracy of the assignment of endonuclease activity to SLFN14, we cloned 104kDa full-length as well as 95, 85, and 65kDa (SLFN14–65kDa) C-terminally truncated His-tagged forms of human protein for expression in *E. coli* cells. Although rabbit SLFN14 contains a 10 kDa C-terminal extension compared to the human homologue, the sequences of both proteins are 78% identical and 86% similar over their entire lengths. All forms were expressed, but only SLFN14–65kDa was found to be soluble in small quantities. We isolated SLFN14–65kDa employing Ni-NTA resin followed by affinity purification through 80S ribosome association during SDG centrifugation. As a control, we used the same purification protocol for the empty vector (Figure 3A). 80S ribosome-bound SLFN14–65kDa, but not a control, after incubation at 37 °C for 12 h caused endonucleolytic rRNA degradation (Figure 3B).

**Sequence and Structure Specificity of SLFN14 in RNA Cleavage.** Next, we determined sequence and structure preferences in RNA cleavage. For that, we utilized HBBmod and GUSmod mRNAs mentioned above. HBBmod mRNA has already been described, whereas GUSmod mRNA comprises the single-stranded 5'-UTR of CAA repeats with a centrally introduced 9 bps stem followed by  $\beta$ -glucuronidase ORF (Figure 3C). After incubation of either mRNA with SLFN14, it was isolated and assayed by primer extension. In both cases, cleavages were distributed along all mRNA, and we did not reveal any sequence or structure preferences (Figure 3D,E, lanes 4 and 5; empty and filled triangles). To compare the cleavage pattern of mRNA in free and ribosome-bound states, we reconstituted 80S initiation and elongation (with one elongation step) ribosomal complexes on HBBmod mRNA from purified components *in vitro* (Figure 3E, lanes 1–3) and treated them with SLFN14. In both complexes, SLFN14 cleaved mRNA almost exclusively at one of many sites observed for free mRNA (Figure 3E, lanes 6–9, empty triangle), which is spatially closest to ribosome-associated SLFN14.

**After rRNA Cleavage by SLFN14, 80S Ribosomes Remain Intact and Active in Translation Whereas Individual Ribosomal Subunits Degrade into Components.** To examine the integrity of ribosome and ribosomal subunits after rRNA cleavage by SLFN14, purified 80S

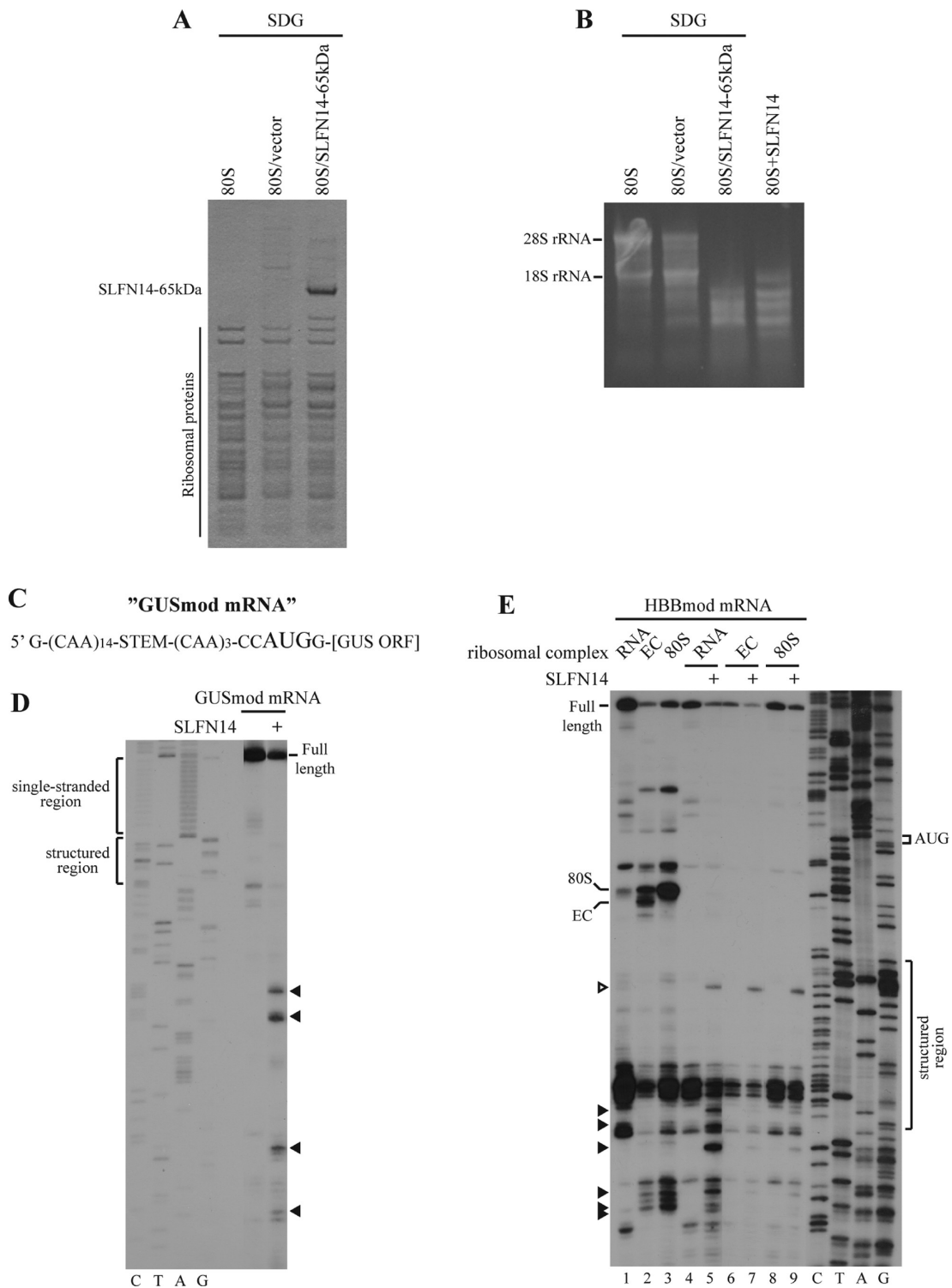


**Figure 3.** Endonucleolytic activity of recombinant human SLFN14–65kDa and sequence and structure specificity of SLFN14 in cleavage of free and ribosome-associated mRNA. (A) Affinity purification of SLFN14–65kDa on 80S ribosomes by centrifugation through SDG assayed by SDS–PAGE and Coomassie staining. (B) rRNA degradation in the SDG-purified 80S/SLFN14–65kDa complex, the 80S/empty vector expression complex, and the empty 80S ribosome after incubation analyzed by DAFGE. Native rabbit SLFN14 is a positive control (lane 4). (C) Structure of GUSmod mRNA. *GUS* is the name of the gene encoding  $\beta$ -glucuronidase protein. (D and E) Endonucleolytic cleavage of free GUSmod mRNA (D), free HBBmod mRNA (E, lanes 4 and 5), and ribosome-bound HBBmod mRNA (E, lanes 6–9) in 80S initiation (80S) and elongation complexes (EC) by SLFN14 assayed by primer extension. Efficiency of formation of ribosomal complexes assembled from purified components *in vitro* analyzed by toeprint (E, lanes 1–3). The empty triangle points to the cleavage position presented in both free and ribosome-associated mRNA. Black triangles indicate cleavage positions in free mRNA only. Positions of full-length cDNA and toeprints corresponding to ribosomal complexes as well as single-stranded and structured regions within mRNAs are indicated. Lanes C, T, A, and G depict corresponding DNA sequences.

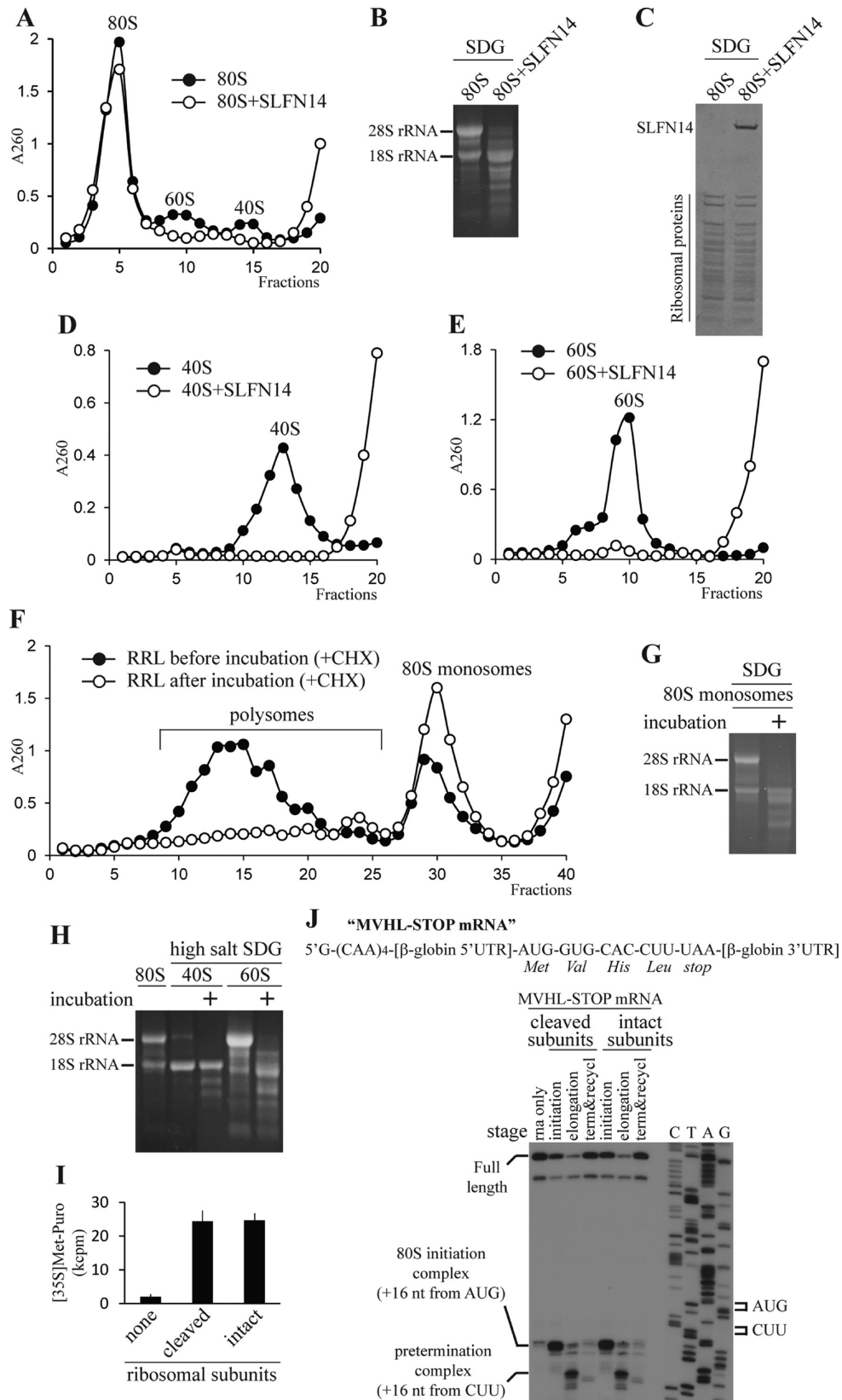


**Figure 4.** Integrity and translation activity of ribosomes and ribosomal subunits after rRNA cleavage by SLFN14. (A) Integrity of 80S ribosomes after incubation with SLFN14 assayed by SDG centrifugation. (B and C) rRNA appearance and protein content, respectively, of 80S ribosomes after SLFN14 treatment and SDG purification analyzed by DAFGE and SDS–PAGE, respectively. (D and E) Degradation of 40S subunits and 60S subunits, respectively, after incubation with SLFN14 assayed by SDG centrifugation. (F) Ribosomal profiling of RRL before and after incubation at 37 °C in the presence of CHX obtained by SDG centrifugation. The total amount of ribosomes was decreased by 26 ± 3% (average ± standard deviation; *n* = 3) after incubation. Upper fractions were omitted for the sake of clarity. (G) rRNA appearance of 80S monosomes after incubation of RRL at 37 °C and ribosomal profiling. (H) rRNA appearance of cleaved 80S ribosome-derived 40S and 60S subunits purified from RRL after



Figure 4. continued

incubation at 37 °C and centrifugation through high-salt SDG. (I) Methionyl-puromycin assay of 80S initiation complex formation with purified intact/cleaved ribosomal subunits. (J) Structure of MVHL-STOP mRNA (top panel). Toeprint analysis of ribosomal complexes at different stages of translation assembled on MVHL-STOP mRNA *in vitro* with purified intact/cleaved ribosomal subunits (bottom). Lanes C, T, A, and G depict the cDNA sequence of MVHL-STOP mRNA. Positions of full-length cDNA and of toeprints corresponding to ribosomal complexes are indicated.

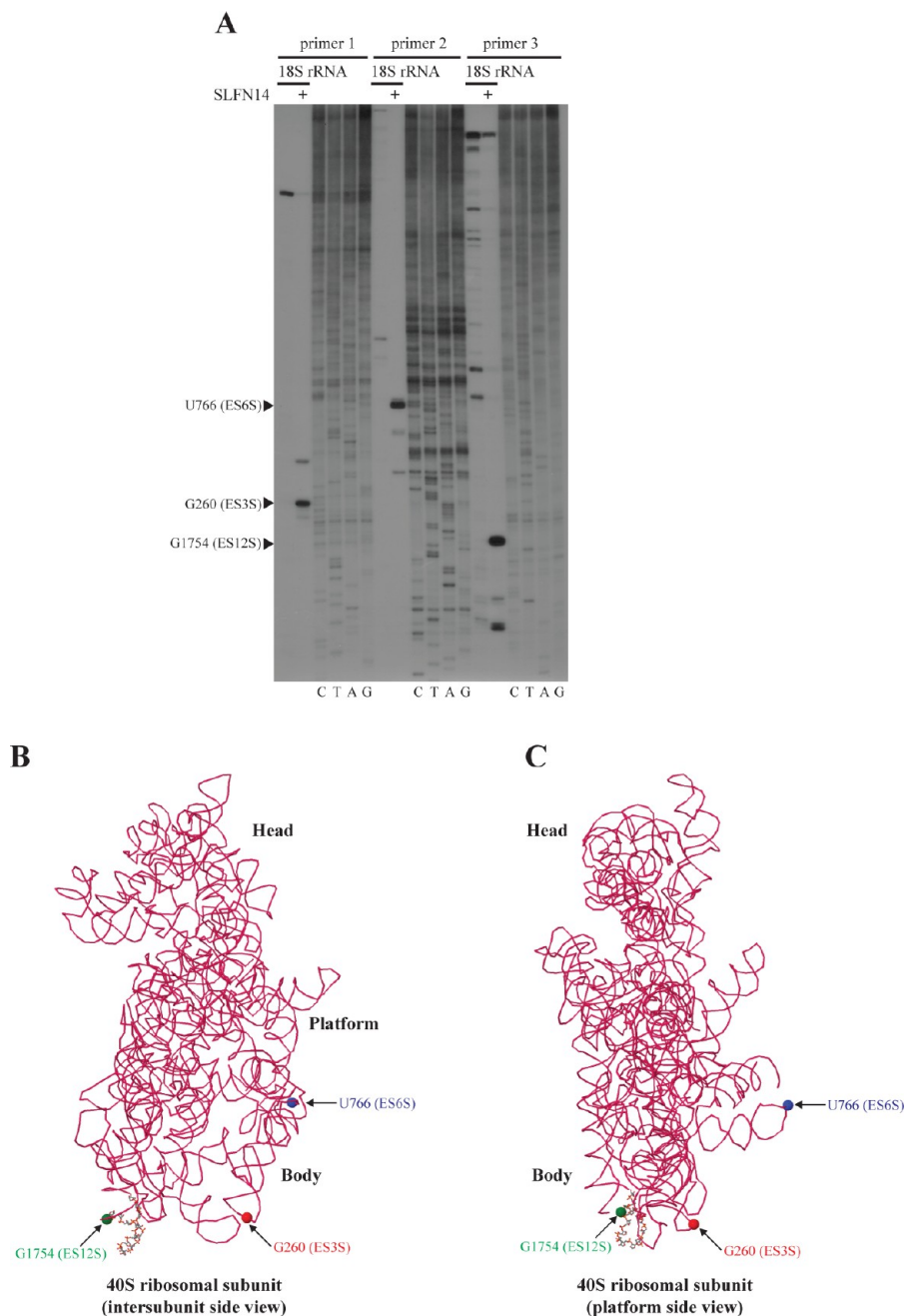


**Figure 5.** Ribosomal position of SLFN14. (A) Identification of prevalent cleavage sites in 18S rRNA after incubation of 40S ribosomal subunits with SLFN14 assayed by primer extension. Black triangles indicate the position and expansion segment location of residues cleaved by SLFN14. Primers 1–3 are described in the Supporting Information. (B and C) Intersubunit side and platform side views, respectively, of 18S rRNA nucleotides cleaved by SLFN14 mapped onto the crystal structure of the *Saccharomyces cerevisiae* 40S subunit (Protein Data Bank entry 3U5B). 18S rRNA (magenta) is shown in backbone representation. Protected nucleotides are colored green, red, and blue.

ribosomes or 40S and 60S subunits were treated with SLFN14 and subjected to SDG centrifugation. 80S ribosomes remain intact in a gradient (Figure 4A), despite rRNA cleavage (Figure 4B), and all ribosomal proteins as well as SLFN14 remain associated (Figure 4C); on the other hand, peaks of 40S and

60S subunits disappear (Figure 4D,E). Probably, cleavage of the RNA-rich intersubunit area, which is hidden in the ribosome, is crucial for ribosomal subunit degradation. To correlate our findings with the fate of ribosomes in RRL, we also subjected RRL, before and after incubation at 37 °C, to SDG

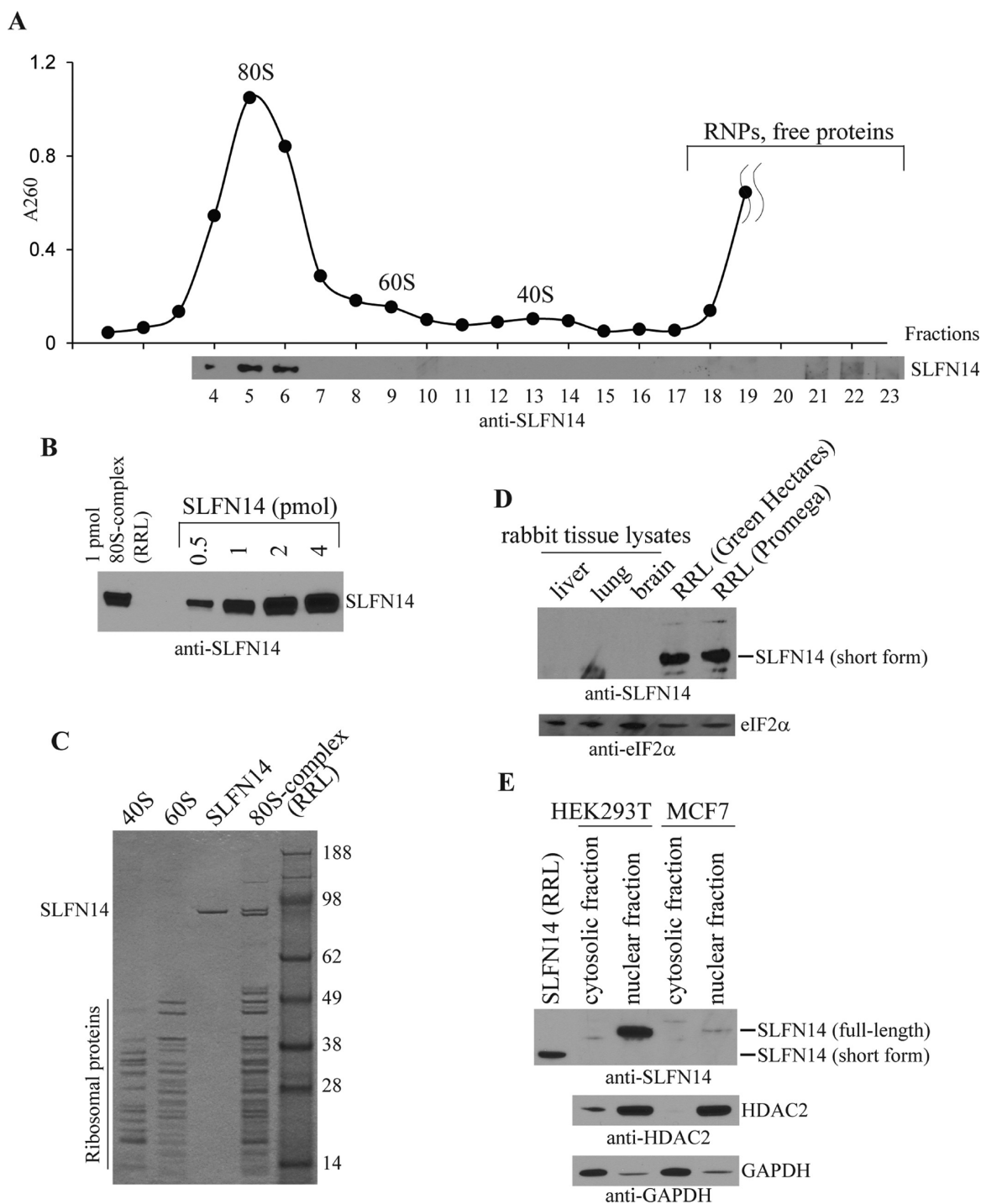


**Figure 6.** SLFN14 protein level and localization in different cell types. (A) SLFN14 distribution (bottom) in the ribosomal profile of mRNA-free RRL (Promega) (top) after SDG centrifugation assayed by immunoblotting. (B and C) Estimation of the SLFN14 to 80S ribosome ratio and SLFN14 abundance, respectively, in the SDG-purified 80S complex from RRL analyzed by immunoblotting and SDS-PAGE, respectively. (D) SLFN14 protein level in two different sources of RRL and rabbit brain, lung, and liver tissue lysates tested by immunoblotting with anti-SLFN14 and anti-eIF2 $\alpha$  (loading control) antibodies. (E) SLFN14 subcellular distribution in HEK293T and MCF7 cells assayed by immunoblotting with anti-SLFN14, anti-HDAC2 (nuclear marker), and anti-GAPDH (cytoplasmic marker) antibodies.

centrifugation. Importantly, incubation was conducted in the presence of cycloheximide (CHX) to exclude polysome runoff. This antibiotic interferes with the translocation step during protein synthesis and, in such a way, blocks the translation elongation stage. As seen from the ribosomal profile, polysomes after incubation separate into monosomes, as a result of polysome-associated mRNA cleavage, and the overall amount

of ribosomes decreases by  $26 \pm 3\%$ , suggesting their partial degradation into components (Figure 4F). In agreement with our findings on purified 80S ribosomes, monosomes remain intact in the SDG profile despite rRNA cleavage (Figure 4G). Next, we decided to test the functional activity of ribosomes in translation after their cleavage in RRL. For that, we incubated RRL overnight at 37 °C, increased the ionic strength to

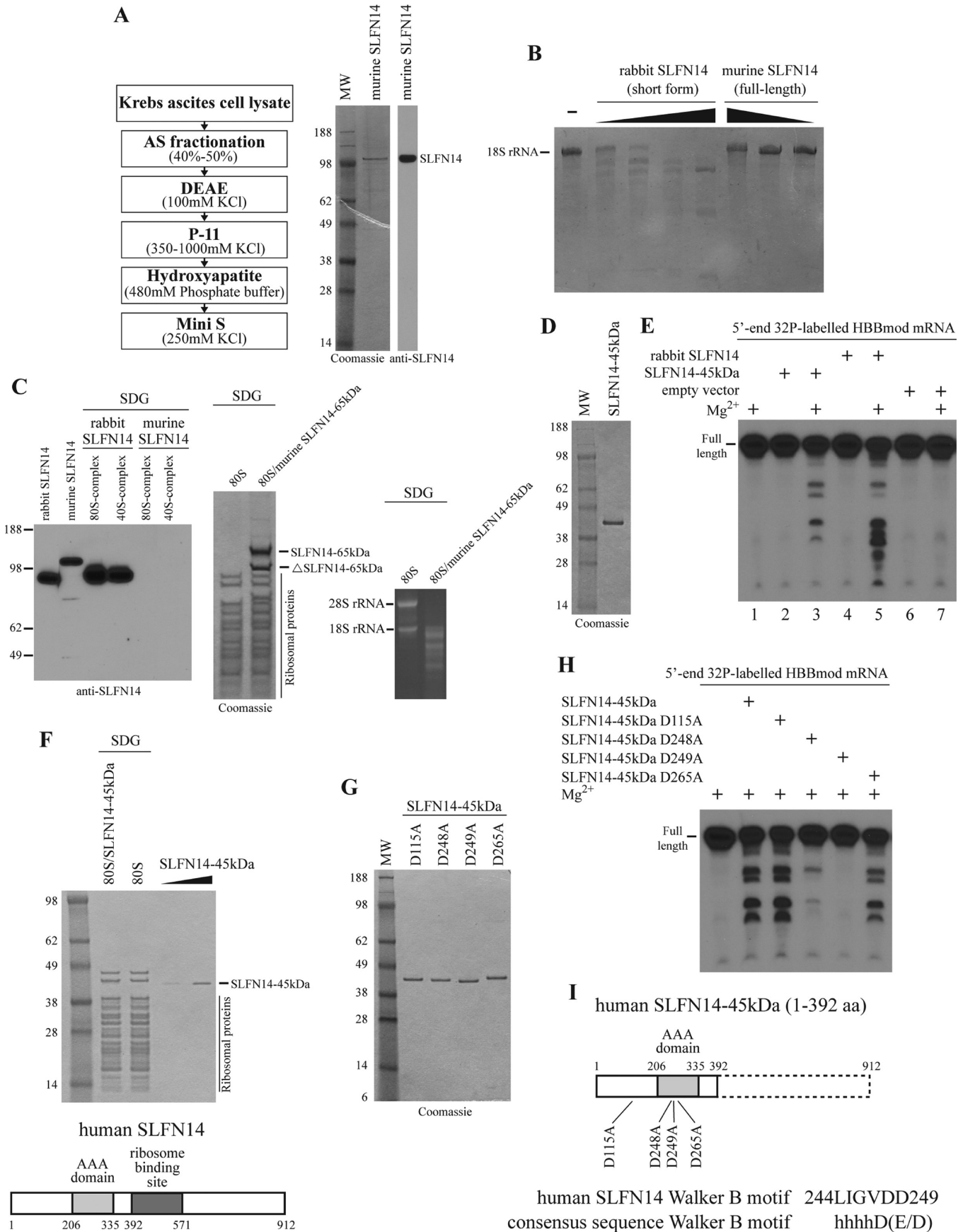


**Figure 7.** Analysis of ribosomal binding and endonucleolytic activities of native murine full-length SLFN14 and mutational analysis of recombinant human SLFN14. (A) Purification scheme for native murine SLFN14 (left). Purified SLFN14 assayed by SDS–PAGE and immunoblotting (right). (B) Endonucleolytic cleavage of 18S rRNA in the 40S subunit by murine full-length and rabbit C-terminally truncated native forms of SLFN14 at

Figure 7. continued

different concentrations tested by denaturing PAGE. (C) Association of native murine and rabbit SLFN14 proteins with 40S subunits and 80S ribosomes assayed by SDG centrifugation and immunoblotting of peak ribosomal fractions (left). Association of recombinant murine SLFN14–65kDa with 80S ribosomes assayed by SDG centrifugation and Coomassie staining (middle). rRNA degradation in the SDG-purified 80S/murine SLFN14–65kDa complex and empty 80S ribosome after incubation analyzed by DAFGE (right). (D) Purified recombinant human SLFN14–45kDa resolved by SDS–PAGE. (E) Endonucleolytic activity of SLFN14–45kDa vs native rabbit SLFN14 analyzed by denaturing PAGE. The concentration of the recombinant or native form in the reaction is 0.9  $\mu$ M or 11 nM, respectively. (F) Ribosomal binding of SLFN14–45kDa tested by SDG centrifugation and SDS–PAGE (top). Location of the ribosomal binding site in human SLFN14 (bottom). (G) Purified recombinant human SLFN14–45kDa mutants resolved by SDS–PAGE. (H) Endonucleolytic activity of different SLFN14–45kDa point mutants assayed by denaturing PAGE. (I) Location of point mutations in SLFN14–45kDa.

separate cleaved ribosomes into subunits, and purified them via centrifugation in high-salt SDG (Figure 4H). Ribosomal subunits with cleaved rRNAs were as active in the methionyl-puromycin assay as intact ones assuming that the translational activity of cleaved ribosomal subunits is not compromised (Figure 4I). To confirm our observation, we compared intact and cleaved ribosomal subunits in all stages of translation (initiation, elongation, termination, and ribosomal recycling) in an *in vitro* reconstituted system employing MVHL-STOP mRNA. This mRNA comprises  $\beta$ -globin 5'-UTR, MVHL-tetrapeptide-encoding ORF and a stop codon, followed by  $\beta$ -globin 3'-UTR (Figure 4J, top panel). In a manner consistent with methionyl-puromycin assay results, we found that the toeprint pattern for 80S initiation and pretermination complexes and the disappearance of toeprint after termination and ribosomal recycling stages were identical for intact and cleaved ribosomal subunits (Figure 4J, bottom panel). Our finding is surprising, but not without precedent. Some strains of bacterial species (for example, *Salmonella*) have naturally fragmented 23S rRNA.

**Ribosomal Position, Cytoplasmic Distribution, and Protein Level of SLFN14 in RRL.** To determine the ribosomal position of SLFN14, we identified cleavage sites of 18S rRNA in the 40S/SLFN14 binary complex. Despite 28S rRNA appearing to be preferentially attacked in ribosomes, it is almost 3 times longer than 18S rRNA. Therefore, we decided to assay only 18S rRNA. SLFN14 cuts at the distal end of expansion segments ES3S, ES6S, and ES12S (Figure 5A), suggesting the approximate location of protein at the low part of the body of the 40S subunit and, presumably, the 80S ribosome (Figure 5B,C). Notably, the existence of extension segments is a feature of the eukaryotic ribosome.

Further, we examined the cytoplasmic distribution of SLFN14 in RRL. We run mRNA-free and, therefore, polysome-free RRL (Promega) in SDG to separate 80S ribosomes, 60S subunits, 40S subunits, and free proteins. To assign peaks, we isolated and analyzed their rRNA content. SLFN14 was found in 80S ribosome-containing fractions, as revealed by immunoblotting of the entire gradient (Figure 6A) (unshaped diffused immunoblotting signals for fractions 21–23 are most likely the background rather than SLFN14), in an equimolar ratio with 80S ribosomes (Figure 6B). Moreover, SLFN14 represents one of the major ribosome-associated proteins in SDS–denaturing polyacrylamide gel electrophoresis (SDS–PAGE) (Figure 6C).

**Nucleated Cells Employ Multiple Levels of Protection from Endonuclease Activity of SLFN14.** Next, we performed the set of experiments to understand how other cell types remain protected from the endonuclease activity of SLFN14. We compared the protein level of SLFN14 in RRL and randomly selected rabbit brain, lung, and liver tissue lysates

by immunoblotting. The level of SLFN14 expression is dramatically higher in RRL than in tissue lysates, where the amount of protein is below the detection limit (Figure 6D). Importantly, SLFN14 is represented exclusively by the C-terminally truncated form in RRL from different sources, eliminating the effect of lysate preparation on the length of the protein. Then, we detected the subcellular localization of SLFN14 in randomly chosen HEK293T and MCF7 (human breast cancer) cells. For that, nuclear and cytoplasmic extracts of cells were prepared and assayed for the presence of protein by immunoblotting. On the basis of the nuclear localization of Schlafens 5, 8, and 9, all long SLFN family members are predicted to be located in the nucleus.<sup>23,24</sup> Consistently, SLFN14 was found solely in nuclear extracts of both cell lines (Figure 6E). Notably, the detected protein in both cell types is the full-length form of SLFN14. Interestingly, reticulocytes and mature erythrocytes are the only non-nucleated cell types in mammals, and this fact may explain the cytoplasmic presence of SLFN14 in RRL. On the basis of our data, we hypothesize that only the short form of protein reveals the endonuclease activity. Therefore, the low expression level, full-length state, and nuclear localization create multiple levels of protection from endonuclease activity of SLFN14 in other rabbit tissues.

**Murine Full-Length SLFN14 neither Cleaves RNA nor Binds to the Ribosome.** Our next aim was to test the hypothesis that full-length SLFN14 is inactive compared to the C-terminally truncated form. Because we could not obtain recombinant full-length SLFN14 in a soluble state, we decided to isolate the endogenous native protein from the available natural source. Therefore, we detected and purified it from the Krebs ascites cell lysate employing the combination of fractionation techniques and chasing the protein by immunoblotting (Figure 7A). Murine full-length SLFN14 is a 102 kDa polypeptide and, like the human form, is highly homologous to rabbit SLFN14. To study the endonucleolytic activity, murine protein at different concentrations was incubated with 40S ribosomal subunits, and 18S rRNA was isolated and assayed by PAGE. In contrast to a rabbit form, it did not cause the cleavage of 18S rRNA (Figure 7B). Further, we asked whether full-length SLFN14, despite the absence of endonucleolytic activity, may still associate with the ribosome and ribosomal subunits. Because of the high adsorption of proteins to the gradient tube and the limited amount of murine SLFN14, we assayed the SDG-purified ribosomal complexes by immunoblotting. Again in contrast to a rabbit short form, the murine full-length homologue bound to neither the 40S subunit nor the 80S ribosome (Figure 7C, left panel). To test whether the murine shorter form of protein can associate with the 80S ribosome, we cloned the 65 kDa C-terminally truncated version of murine SLFN14 (murine SLFN14–65kDa), similar to rabbit SLFN14–65kDa, for the expression in *E. coli* cells. Because

murine SLFN14–65kDa was found to be soluble in small quantities after expression, we assayed its interaction with the 80S ribosome employing the same protocol that was used for rabbit SLFN14–65kDa. As expected, murine SLFN14–65 kDa along with its even shorter form ( $\Delta$ SLFN14–65kDa) strongly binds to the 80S ribosome as revealed by SDG centrifugation (Figure 7C, middle panel). Moreover, murine SLFN14–65kDa causes the endonucleolytic cleavage of both rRNAs after incubation of the SDG-purified 80S/murine SLFN14–65kDa complex (Figure 7C, right panel). In conclusion, the endonucleolytic activity and the ribosomal binding site of SLFN14 are hidden in the presence of the C-terminal part of the protein. It would be interesting to know the mechanism underlying the appearance of the C-terminally truncated form, but this question is beyond the scope of this work.

**Mutational Analysis of SLFN14 Revealed the Ribosomal Binding Site and the Aspartate Essential for the Endonucleolytic Activity of Protein.** To study the catalytic activity of SLFN14, we employed the mutational analysis. Because the only soluble recombinant form, SLFN14–65kDa, was available in a limited amount, in the next clone we removed an additional 20 kDa from the C-terminus. SLFN14–45kDa was highly expressed and completely soluble. We purified it until high homogeneity employing the combination of Ni-NTA affinity resin and FPLC on MonoS column techniques (Figure 7D). Like the native protein, SLFN14–45kDa caused the endonucleolytic cleavage of RNA in a  $Mg^{2+}$ -dependent manner, but much less efficiently, indicating that the active center is partially compromised (Figure 7E, lanes 1–5). To rule out the potential cleavage activity associated with the copurified bacterial endogenous proteins, we performed the expression and protein purification protocols for the empty vector exactly as for SLFN14–45kDa. Compared to native and recombinant SLFN14 forms, we did not obtain RNA degradation in the presence or absence of  $Mg^{2+}$  ions for the empty vector expression control (Figure 7E, lanes 6 and 7). Interestingly, in contrast to SLFN14–65kDa, SLFN14–45kDa could not associate with the 80S ribosome, suggesting the location of the ribosomal binding site within 179 amino acids beside the AAA domain to the C-terminus (Figure 7F). Thus, SLFN14–45kDa was chosen as the basis for the point mutation analysis. Like well-characterized RNase L, Dicer, Ago2, and SMG6, SLFN14 is the  $Mg^{2+}$ - and  $Mn^{2+}$ -dependent and ATP-independent enzyme. It is shown that  $Mg^{2+}$  ion is coordinated by one Asp and one Asn in the catalytic center of RNase L,<sup>25</sup> by two Asp and two Gln residues in Dicer,<sup>26,27</sup> by an Asp-Asp-His motif in Ago2,<sup>28</sup> and by one Asp in the essential Asp-Asp-Asp motif in SMG6.<sup>29</sup> Therefore, Asp is one of the key amino acids in the active center of these enzymes. We identified 10 Asp residues within SLFN14–45kDa, which are conserved among mammals. Importantly, two Asp residues belong to the Walker B motif 244LIGVDD249, which is the signature motif of the AAA domain. It is well-known that the Walker B motif, which contains the consensus sequence hhhhD(E/D), where h is a hydrophobic acid, is involved in  $Mg^{2+}$  coordination and ATP hydrolysis. Interestingly, several AAA proteins are not active as ATPases, and some do not even bind ATP. Therefore, we cloned, expressed in *E. coli*, and purified four Asp single-point mutants. We substituted each Asp in the Walker B motif and randomly selected for the mutation two other conservative ones. RNA degradation analysis revealed that the D249A mutant was inactive and the activity of the D248A mutant was strongly decreased, whereas others caused the cleavage with a

similar characteristic pattern (Figure 7G–I). Thus, Asp249, which probably coordinates the  $Mg^{2+}$  ion, is essential for the endonucleolytic activity of SLFN14. Importantly, because endonuclease activity has not previously been reported for AAA ATPases, it is equally possible that Asp249 could be required for the structural integrity of the catalytic center or even the entire protein.

## DISCUSSION

In an attempt to identify the endoribonuclease involved in the no-go decay, we employed the RRL fractionation approach coupled with testing of intermediate fractions in examining the ability to cause the endonucleolytic cleavage of mRNA in the reconstituted stalled EC. This approach resulted in the purification of the C-terminally truncated form of SLFN14, which is ~20 kDa shorter than the 114 kDa full-length rabbit protein. Interestingly, immunoblotting analysis of RRL from different sources did not reveal the presence of the full-length form of the enzyme. The function of SLFN14 is completely unknown, and there has been no work concerning its characterization at a biochemical or cellular level published. SLFN14 belongs to the Schlafen protein family based on the presence of specific slfn signature motifs.<sup>18,19</sup> The SLFN family is limited to mammals and represents a diverse group of proteins with essential sequence variability among species. For example, there are eight murine SLFNs and six human SLFNs,<sup>30</sup> suggesting that they may have different species specific functions. The precise role of SLFN proteins in the cell remains to be identified; however, several members of the family are found to be involved in development, cell proliferation, and immune response.<sup>30</sup> SLFN14 contains the AAA domain at the N-terminus and the motif, homologous to the superfamily of DNA/RNA helicases, at the C-terminus. AAA proteins, where AAA is the abbreviation for ATPase associated with diverse cellular activities, make up the large and functionally diverse protein family involved in a wide variety of processes such as DNA replication, protein degradation, membrane fusion, microtubule severing, peroxisome biogenesis, signal transduction, and the regulation of gene expression. Notably, SLFN14 possesses the shortened 129-amino acid AAA domain, compared to the 200–250-amino acid regular one, without several signature motifs. For example, the Walker A motif, which is involved in ATP binding, is absent. In contrast to other SLFN members, SLFN14 is highly homologous among all species where it is present, for example, in rabbit, human, chimpanzee, cow, rat, dog, and mouse.

In the control experiment, native rabbit SLFN14 caused the endonucleolytic cleavage of mRNA in the proximity of the stalled EC. Surprisingly, this enzyme also resulted in multiple cleavages all along mRNA in the binary SLFN14/mRNA complex in a ribosome-independent manner. Because SLFN14 is enriched with RSW, we tested its potential effect on the stability of rRNA in RRL and found that both 28S and 18S rRNAs became fully degraded with the formation of the characteristic endonucleolytic cleavage pattern after the incubation of RRL for 12 h at 37 °C. Absolutely the same final degradation pattern was obtained after the incubation for 12 h of the 80S/SLFN14 binary complex with the equimolar ratio of components assuming that SLFN14 is indeed involved in the rRNA cleavage in RRL. Consistently, it also cut rRNA when it was mixed with individual ribosomal subunits, producing again the characteristic degradation pattern. To confirm the universality of endonucleolytic activity, SLFN14

was assayed in the presence of different types of RNA. It caused the cleavage of all tested mRNAs and tRNAs. In agreement with the enrichment in RSW, SLFN14 binds to the ribosome and both ribosomal subunits, and the association is ATP-independent. Ribosomal binding unambiguously indicates the role of this protein in the translation regulation. Like those of well-characterized RNase L, Dicer, Ago2, and SMG6 endoribonucleases, the nuclease activity of SLFN14 is  $Mg^{2+}$ - and  $Mn^{2+}$ -dependent and ATP-independent. Moreover, despite the presence of the AAA domain, SLFN14 does not hydrolyze ATP and the hydrolysis is not stimulated by either the ribosome or RNA. It is not surprising, because some AAA proteins do not even bind ATP. Because of the high structural diversity, the nuclease domains responsible for the endonucleolytic activity of many enzymes are not identified yet, and this is the case for SLFN14. However, like previously mentioned endoribonucleases, SLFN14 shares the same divalent ion-mediated mechanism of phosphodiester bond activation in the catalytic center of the protein.

To confirm the correct assignment of the endonucleolytic activity to SLFN14, we purified from *E. coli* the recombinant human SLFN14–65kDa, which represents the C-terminally truncated form of protein. Unfortunately, we could not obtain a longer form in a soluble state after expression. This protein efficiently binds to the ribosome and causes RNA degradation, showing that the C-terminal third of SLFN14 is dispensable for both activities. To test the sequence and structure specificities of SLFN14 in the cleavage of RNA, we assayed the enzyme in the presence of model mRNAs with the definite single-stranded and structured regions. We did not detect any sequence and structure preferences. We assume that the hydrolysis takes place in the energetically favorable phosphodiester bonds, which, in turn, are defined by the tertiary structure of RNA. In contrast to multiple cleavages of the free mRNA, ribosome-bound SLFN14 cuts mRNA in the 80S initiation complex and different elongation complexes predominantly at the spatially closest energetically favorable site. Because SLFN14 in association with the ribosome also cleaves rRNAs, we identified its ribosomal binding site employing the primer extension technique. In the binary 40S/SLFN14 complex, the enzyme cuts 18S rRNA at the distal end of expansion segments ES3S, ES6S, and ES12S, indicating its location at the low part of the body of the 40S subunit and likely at the corresponding low part of the 60S subunit in the 80S ribosome. Interestingly, expansion segments are absent in prokaryotic ribosomes, and their functions mainly remain obscure.<sup>31</sup> After rRNA cleavage of individual ribosomal subunits, they both degrade into components. In contrast, after rRNA cleavage of 80S ribosomes, the last remain undegraded. Interestingly, the simultaneous presence of several cuts in rRNA does not influence the integrity of the 80S ribosome. Analysis of the intracellular distribution of SLFN14 in RRL revealed that the enzyme is associated with ribosomes and is absent in the free form in the cytoplasm. Moreover, it is overexpressed and is presented in an equimolar ratio with ribosomes, indicating the enormous content of this endoribonuclease in reticulocytes. As a result, SLFN14 is one of few major ribosome-associated proteins in RRL. In a manner consistent with the high ribosomal affinity, SLFN14 in RRL cleaves first of all ribosomal and ribosome-associated RNA but potentially may cleave any type of RNA, resulting in the separation of polysomes into monosomes. Surprisingly, cleaved 80S ribosomes are active in all stages of translation (initiation, elongation, termination, and

ribosomal recycling). Because the rRNA-rich intersubunit area remains hidden in the ribosome, the integrity and the catalytic centers involved in translation activity of ribosomes, obviously, are not compromised.

We also tried to understand the mechanism by which other cell types preserve the RNA integrity from the endonucleolytic activity of SLFN14. We found that in contrast to reticulocytes, the SLFN14 level is below the detection limit in brain, lung, and liver tissues. Our data are supported by two other reports in which the relative level of SLFN14 expression was found to be very low in primary normal human melanocytes and malignant melanoma cells<sup>23</sup> and was shown to be very low or even below the detection level in HEK293, HEK293T, HeLa, CEM, and Jurkat cells.<sup>20</sup> Our analysis of the subcellular distribution in nucleated cells revealed that SLFN14 is located in the nucleus and is represented by the full-length form in HEK293T and MCF7 cells. Thus, the low expression level and nuclear localization may create the barrier for RNA degradation by SLFN14. Consistently, we did not detect the RNA cleavage after incubation of HEK293T lysate, although the latter contains SLFN14 as revealed by immunoblotting. Moreover, because SLFN14 is represented by the full-length version in tested nucleated cells and by the C-terminally truncated version in RRL, we assign the endonuclease activity to the short form of the protein. It is well-known that some members of caspases, the family of cysteine proteases, become activated by the proteolytic cleavage of their pro forms. To test our hypothesis, we purified native murine full-length SLFN14 from Krebs ascites cell lysate. In contrast to the short form, the full-length SLFN14 did not bind to the ribosome and ribosomal subunits and did not cleave the rRNA, confirming our hypothesis.

Finally, we employed the mutational analysis to identify the ribosomal binding site and to gain insights into the organization of the catalytic center of SLFN14. We located the ribosomal binding site within 179 amino acids in the central part of the protein beside the AAA domain to the C-terminus. Like those of well-characterized RNase L, Dicer, Ago2, and SMG6 endoribonucleases, the activity of SLFN14 strictly depends on  $Mg^{2+}$  and  $Mn^{2+}$  ions. Aspartic acid plays the essential role of the coordination of divalent ion in the catalytic center of all four mentioned endoribonucleases. Analyzing different point mutants of SLFN14, we found that Asp249 is critical for its endonucleolytic activity. Asp249 is located in the Walker B motif, which is the signature motif of the AAA domain. Interestingly, the Walker B motif of SLFN14 with the sequence 244LIGVDD249 belongs to the minor subgroup of Walker B motifs within AAA proteins with the consensus sequence hhhhD(E/D), where h is a hydrophobic acid. Generally, the last amino acid of the consensus sequence is glutamate, and only few members of AAA proteins contain aspartate instead. Another important detail is that the AAA domain of SLFN14 is substantially shorter than the regular AAA domain of AAA proteins (129 amino acids vs 200–250 amino acids), and as a result, some signature motifs are missing. Thus, we assume that the evolutionarily modified AAA domain of SLFN14, which originally couples ATP hydrolysis with conformational changes of protein, lost ATP hydrolyzing activity but retained the ability to coordinate  $Mg^{2+}$  ion and currently constitutes the part of the catalytic center of the enzyme. However, because endonuclease activity has not been ascribed so far to the AAA domain, it is equally possible that Asp249 is important for the structural integrity of the catalytic center or even the entire protein.

On the basis of our data, we suggest several possible target processes for SLFN14. The first proposed process is limited to reticulocytes. Mammalian reticulocytes do not have a cell nucleus but contain a network of ribosomes and the endoplasmic reticulum.<sup>32,33</sup> They become fully matured erythrocytes as their ribosomes are degraded by intracellular enzymes. In particular, polysomes separate into monosomes, reduce in number, and disappear, and the total RNA content decreases in parallel.<sup>34,35</sup> The rate of RNA degradation during reticulocyte maturation *in vitro* at 37 °C is 4% per hour. Additionally, ribosomes and ribosome-associated RNA are degraded at a rate greater than that of free RNA.<sup>36</sup> To date, reticulocyte maturation and, particularly, RNA degradation have been studied at the cellular level, but the mechanism is still unknown. Several reports of the characterization of ribonucleases responsible for RNA degradation have been presented, but their data are contradictory to each other.<sup>37–40</sup> We found that SLFN14 binds specifically and exceptionally to ribosomes and ribosomal subunits and cleaves ribosomal and ribosome-associated RNA. These results are in a good agreement with the preferential degradation of ribosomes and ribosome-associated RNA rather than free RNA during intact rabbit reticulocyte maturation *in vitro*.<sup>36</sup> Ribosomal binding of SLFN14 is a good strategy for the targeted degradation of actively translating mRNAs. This approach may help reticulocytes save energy for other cellular processes because the energy production is also terminated during reticulocyte maturation.<sup>41</sup> Importantly, the requirement to degrade different RNAs may explain the sequence nonspecificity of SLFN14. We determined that incubation of SLFN14 with ribosomes at a physiological ratio results in complete rRNA degradation in only 12 h, which is also consistent with the low RNA degradation rate in intact reticulocytes. RNA degradation along with clearance from many cellular organelles and the lack of DNA in mammalian reticulocytes are unique among vertebrates. As a result, mammalian erythrocytes are optimized for oxygen transport. Therefore, the *Slfn14* gene could originate in the evolution of mammals presumably to contribute to the efficiency of erythrocytes. Second, SLFN14 could be involved in the antiviral host response. It is well-known that RNase L is an interferon (IFN)-activated endoribonuclease, which destroys total cellular RNA, including viral RNA. The expression of several members of the Schlafen protein family is induced by IFN- $\alpha$  in mice.<sup>42</sup> Although SLFN14 was not tested, all *Slfn* genes are located in the same chromosomal locus at least in mouse, rat, and human,<sup>30</sup> and the expression of SLFN14 should be also upregulated in response to the IFN stimulus. Therefore, upon activation, SLFN14 may play a role in the clearance of total cellular RNA similar to that of RNase L. Finally, the enzyme may be the missing endoribonuclease in the NGD pathway. To date, we have insufficient experimental data to confirm or rule out this guess. Despite our suggestions, the real process for the activity of SLFN14 is yet to be identified. However, because only a few endoribonucleases involved in mammalian translation control have been characterized so far, the discovery and biochemical analysis of novel endoribonuclease SLFN14 expand our knowledge of the role of this class of enzymes in the ribosome-mediated processes.

## ■ ASSOCIATED CONTENT

### 📄 Supporting Information

Descriptions of plasmid construction, cell extracts, and denaturing agarose/formaldehyde gel electrophoresis

(DAFGE) and detailed protocols for all experimental procedures. The Supporting Information is available free of charge on the ACS Publications website at DOI: 10.1021/acs.biochem.5b00302.

## ■ AUTHOR INFORMATION

### Corresponding Authors

\*Department of Cell Biology, SUNY Downstate Medical Center, 450 Clarkson Ave., Box 44, Brooklyn, NY 11203. E-mail: andrey.pisarev@downstate.edu. Telephone: (718) 270-1143. Fax: (718) 270-2656.

\*Department of Cell Biology, SUNY Downstate Medical Center, 450 Clarkson Ave., Box 44, Brooklyn, NY 11203. E-mail: vera.pisarev@downstate.edu. Telephone: (718) 270-1143. Fax: (718) 270-2656.

### Funding

This work was supported by National Institutes of Health Grant GM097014 to A.V.P.

### Notes

The authors declare no competing financial interest.

## ■ ACKNOWLEDGMENTS

We thank Louie Semaan for the helpful discussion.

## ■ ABBREVIATIONS

5'-UTR, 5'-untranslated region; CHX, cycloheximide; DAFGE, denaturing agarose/formaldehyde gel electrophoresis; EC, elongation complex; ER, endoplasmic reticulum; IFN, interferon; mRNA, messenger RNA; NGD, no-go decay; NMD, nonsense-mediated decay; NSD, nonstop decay; ORF, open reading frame; PAGE, polyacrylamide gel electrophoresis; RISC, RNA-induced silencing complex; RRL, rabbit reticulocyte lysate; RSW, ribosomal salt wash; SDG, sucrose density gradient.

## ■ REFERENCES

- (1) Li, W. M., Barnes, T., and Lee, C. H. (2010) Endoribonucleases: Enzymes gaining spotlight in mRNA metabolism. *FEBS J.* 277, 627–641.
- (2) Tomecki, R., and Dziembowski, A. (2010) Novel endoribonucleases as central players in various pathways of eukaryotic RNA metabolism. *RNA* 116, 1692–1724.
- (3) Walter, P., and Ron, D. (2011) The unfolded protein response: From stress pathway to homeostatic regulation. *Science* 334, 1081–1086.
- (4) Hollien, J., and Weissman, J. S. (2006) Decay of endoplasmic reticulum-localized mRNAs during the unfolded protein response. *Science* 313, 104–107.
- (5) Cunningham, K. S., Hanson, M. N., and Schoenberg, D. R. (2001) Polysomal ribonuclease 1 exists in a latent form on polysomes prior to estrogen activation of mRNA decay. *Nucleic Acids Res.* 29, 1156–1162.
- (6) Yang, F., Peng, Y., Murray, E. L., Otsuka, Y., Kedersha, N., and Schoenberg, D. R. (2006) Polysome-bound endonuclease PMR1 is targeted to stress granules via stress-specific binding to TIA-1. *Mol. Cell Biol.* 26, 8803–8813.
- (7) Barnes, T., Kim, W. C., Mantha, A. K., Kim, S. E., Izumi, T., Mitra, S., and Lee, C. H. (2009) Identification of apurinic/aprimidinic endonuclease 1 (APE1) as the endoribonuclease that cleaves c-myc mRNA. *Nucleic Acids Res.* 37, 3946–3958.
- (8) Claverie-Martin, F., Wang, M., and Cohen, S. N. (1997) ARD-1 cDNA from human cells encodes a site-specific single-strand endoribonuclease that functionally resembles *Escherichia coli* RNase E. *J. Biol. Chem.* 272, 13823–13828.

- (9) Tourriere, H., Gallouzi, I. E., Chebli, K., Capony, J. P., Mouaikel, J., van der Geer, P., and Tazi, J. (2001) RasGAP-associated endoribonuclease G3Bp: Selective RNA degradation and phosphorylation-dependent localization. *Mol. Cell. Biol.* 21, 7747–7760.
- (10) Doma, M. K., and Parker, R. (2007) RNA quality control in eukaryotes. *Cell* 131, 660–668.
- (11) Isken, O., and Maquat, L. E. (2007) Quality control of eukaryotic mRNA: Safeguarding cells from abnormal mRNA function. *Genes Dev.* 21, 1833–1856.
- (12) Nicholson, P., Yepiskoposyan, H., Metze, S., Zamudio Orozco, R., Kleinschmidt, N., and Muhlemann, O. (2010) Nonsense-mediated mRNA decay in human cells: Mechanistic insights, functions beyond quality control and the double-life of NMD factors. *Cell. Mol. Life Sci.* 67, 677–700.
- (13) Doma, M. K., and Parker, R. (2006) Endonucleolytic cleavage of eukaryotic mRNAs with stalls in translation elongation. *Nature* 440, 561–564.
- (14) Schwarz, D. A., Katayama, C. D., and Hedrick, S. M. (1998) Schlafen, a new family of growth regulatory genes that affect thymocyte development. *Immunity* 9, 657–668.
- (15) Pisareva, V. P., Pisarev, A. V., Komar, A. A., Hellen, C. U., and Pestova, T. V. (2008) Translation initiation on mammalian mRNAs with structured 5'UTRs requires DExH-box protein DHX29. *Cell* 135, 1237–1250.
- (16) Pisarev, A. V., Skabkin, M. A., Pisareva, V. P., Skabkina, O. V., Rakotondrafara, A. M., Hentze, M. W., Hellen, C. U., and Pestova, T. V. (2010) The role of ABCE1 in eukaryotic posttermination ribosomal recycling. *Mol. Cell* 37, 196–210.
- (17) Pestova, T. V., Lomakin, I. B., Lee, J. H., Choi, S. K., Dever, T. E., and Hellen, C. U. (2000) The joining of ribosomal subunits in eukaryotes requires eIF5B. *Nature* 403, 332–335.
- (18) Geserick, P., Kaiser, F., Klemm, U., Kaufmann, S. H., and Zerrahn, J. (2004) Modulation of T cell development and activation by novel members of the Schlafen (slfn) gene family harbouring an RNA helicase-like motif. *Int. Immunol.* 16, 1535–1548.
- (19) Brady, G., Boggan, L., Bowie, A., and O'Neill, L. A. (2005) Schlafen-1 causes a cell cycle arrest by inhibiting induction of cyclin D1. *J. Biol. Chem.* 280, 30723–30734.
- (20) Li, M., Kao, E., Gao, X., Sandig, H., Limmer, K., Pavon-Eternod, M., Jones, T. E., Landry, S., Pan, T., Weitzman, M. D., and David, M. (2012) Codon-usage-based inhibition of HIV protein synthesis by human schlafen 11. *Nature* 491, 125–128.
- (21) Patel, V. B., Yu, Y., Das, J. K., Patel, B. B., and Majumdar, A. P. (2009) Schlafen-3: A novel regulator of intestinal differentiation. *Biochem. Biophys. Res. Commun.* 388, 752–756.
- (22) Berger, M., Krebs, P., Crozat, K., Li, X., Croker, B. A., Siggs, O. M., Popkin, D., Du, X., Lawson, B. R., Theofilopoulos, A. N., Xia, Y., Khovananth, K., Moresco, E. M., Satoh, T., Takeuchi, O., Akira, S., and Beutler, B. (2010) An Slfn2 mutation causes lymphoid and myeloid immunodeficiency due to loss of immune cell quiescence. *Nat. Immunol.* 11, 335–343.
- (23) Katsoulidis, E., Mavrommatis, E., Woodard, J., Shields, M. A., Sassano, A., Carayol, N., Sawicki, K. T., Munshi, H. G., and Platanius, L. C. (2010) Role of interferon  $\alpha$  (IFN $\alpha$ )-inducible Schlafen-5 in regulation of anchorage-independent growth and invasion of malignant melanoma cells. *J. Biol. Chem.* 285, 40333–40341.
- (24) Neumann, B., Zhao, L., Murphy, K., and Gonda, T. J. (2008) Subcellular localization of the Schlafen protein family. *Biochem. Biophys. Res. Commun.* 370, 62–66.
- (25) Huang, H., Zeqiraj, E., Dong, B., Jha, B. K., Duffy, N. M., Orlicky, S., Thevakumaran, N., Talukdar, M., Pillon, M. C., Ceccarelli, D. F., Wan, L. C., Juang, Y. C., Mao, D. Y., Gaughan, C., Brinton, M. A., Perelygin, A. A., Kourinov, I., Guarne, A., Silverman, R. H., and Sicheri, F. (2014) Dimeric Structure of Pseudokinase RNase L Bound to 2–5A Reveals a Basis for Interferon-Induced Antiviral Activity. *Mol. Cell* 53, 221–234.
- (26) Gan, J., Tropea, J. E., Austin, B. P., Court, D. L., Waugh, D. S., and Ji, X. (2006) Structural insight into the mechanism of double-stranded RNA processing by ribonuclease III. *Cell* 124, 355–366.
- (27) Jinek, M., and Doudna, J. A. (2009) A three-dimensional view of the molecular machinery of RNA interference. *Nature* 457, 405–412.
- (28) Rivas, F. V., Tolia, N. H., Song, J. J., Aragon, J. P., Liu, J., Hannon, G. J., and Joshua-Tor, L. (2005) Purified Argonaute2 and an siRNA form recombinant human RISC. *Nat. Struct. Mol. Biol.* 12, 340–349.
- (29) Glavan, F., Behm-Ansmant, I., Izaurralde, E., and Conti, E. (2006) Structures of the PIN domains of SMG6 and SMG5 reveal a nuclease within the mRNA surveillance complex. *EMBO J.* 25, 5117–5125.
- (30) Bustos, O., Naik, S., Ayers, G., Casola, C., Perez-Lamigueiro, M. A., Chippindale, P. T., Pritham, E. J., and de la Casa-Esperón, E. (2009) Evolution of the Schlafen genes, a gene family associated with embryonic lethality, meiotic drive, immune processes and orthopoxvirus virulence. *Gene* 447, 1–11.
- (31) Ben-Shem, A., Garreau de Loubresse, N., Melnikov, S., Jenner, L., Yusupova, G., and Yusupov, M. (2011) The structure of the eukaryotic ribosome at 3.0 Å resolution. *Science* 334, 1524–1529.
- (32) Baldini, M., and Pannacchioli, I. (1960) The maturation rate of reticulocytes. *Blood* 15, 614–629.
- (33) Stryckmans, P. A., Cronkite, E. P., Giacomelli, G., Schiffer, L. M., and Schnappaut, H. P. (1968) The maturation and fate of reticulocytes after in vitro labelling with tritiated amino acids. *Blood* 31, 33–43.
- (34) Muto, K., Mizuno, D., and Goto, S. (1979) In vivo degradation of rat globin messenger RNA during maturation of reticulocytes. *J. Biochem.* 86, 391–401.
- (35) Glowacki, E. R., and Millette, R. L. (1965) Polyribosomes and the loss of hemoglobin synthesis in the maturing reticulocyte. *J. Mol. Biol.* 11, 116–127.
- (36) Burka, E. R. (1969) Characteristic of RNA degradation in the erythroid cell. *J. Clin. Invest.* 48, 1266–1272.
- (37) Adachi, K., Nagano, K., Nakao, T., and Nakao, M. (1964) Purification and characterization of ribonuclease from rabbit reticulocytes. *Biochim. Biophys. Acta* 92, 59–70.
- (38) Stavys, L., Feldman, M., and Elson, D. (1964) On ribonuclease activity in reticulocyte ribosomes. *Biochim. Biophys. Acta* 91, 606–611.
- (39) Farkas, W., and Marks, P. A. (1968) Partial purification and properties of a ribonuclease from rabbit reticulocytes. *J. Biol. Chem.* 243, 6464–6473.
- (40) Rowley, P. T., and Morris, J. A. (1967) Protein synthesis in the maturing reticulocyte. *J. Biol. Chem.* 242, 1533–1540.
- (41) Gronowicz, G., Swift, H., and Steck, T. L. (1984) Maturation of the reticulocyte in vitro. *J. Cell Sci.* 71, 177–197.
- (42) Mavrommatis, E., Arslan, A. D., Sassano, A., Hua, Y., Kroczyńska, B., and Platanius, L. C. (2013) Expression and regulatory effects of murine Schlafen (Slfn) genes in malignant melanoma and renal cell carcinoma. *J. Biol. Chem.* 288, 33006–33015.